

## A Detailed Study of Strange Particle Production in $e^+e^-$ Annihilation at High Energy

TASSO Collaboration

M. Althoff, W. Braunschweig, F.J. Kirschfink,  
K. Lübelmeyer, H.-U. Martyn, P. Roskamp,  
D. Schmitz, H. Siebke, W. Wallraff  
I. Physikalisches Institut der RWTH, D-5100 Aachen,  
Federal Republic of Germany<sup>a</sup>

J. Eisenmann, H.M. Fischer, H. Hartmann,  
A. Joks, G. Knop, H. Kolanoski, H. Kück,  
V. Mertens, R. Wedemeyer  
Physikalisches Institut der Universität, D-5300 Bonn,  
Federal Republic of Germany<sup>a</sup>

B. Foster  
H.H. Wills Physics Laboratory, University, Bristol BS 8 1 TL, UK<sup>b</sup>

A. Eskreys<sup>1</sup>, K. Gather, M. Hildebrandt,  
H. Hultschig, P. Joos, U. Kötz, H. Kowalski,  
A. Ladage, B. Löhr, D. Lüke, P. Mättig, D. Notz,  
R.J. Nowak<sup>2</sup>, J. Pyrlík, E. Ronat<sup>3</sup>, M. Rushton,  
W. Schütte, D. Trines, T. Tymieniecka<sup>2</sup>, G. Wolf,  
G. Yekutieli<sup>3</sup>, Ch. Xiao<sup>7</sup>  
Deutsches Elektronen-Synchrotron DESY, D-2000 Hamburg,  
Federal Republic of Germany

R. Fohrmann, E. Hilger, T. Kracht, H.L. Krasemann,  
P. Leu, E. Lohrmann, D. Pandoulas, G. Poelz,  
K.U. Pösnecker, B.H. Wiik  
II. Institut für Experimentalphysik der Universität,  
D-2000 Hamburg, Federal Republic of Germany<sup>a</sup>

R. Beuselinck, D.M. Binnie, A.J. Campbell<sup>4</sup>,  
P.J. Dornan, D.A. Garbutt, C. Jenkins, T.D. Jones,  
W.G. Jones, J. McCardle, J.K. Sedgbeer,  
J. Thomas, W.A.T. Wan Abdullah<sup>8</sup>  
Department of Physics, Imperial College, London SW 7 2 BZ, UK<sup>b</sup>

K.W. Bell<sup>9</sup>, M.G. Bowler, P. Bull, R.J. Cashmore,  
P.E.L. Clarke, P. Dauncey, R. Devenish,  
P. Grossmann, C.M. Hawkes, S.L. Lloyd, D. Mellor,  
C. Youngman  
Department of Nuclear Physics, University,  
Oxford OX 1 3 RH, UK<sup>b</sup>

G.E. Forden, J.C. Hart, J. Harvey, D.K. Hasell,  
D.H. Saxon, P.L. Woodworth<sup>5</sup>  
Rutherford Appleton Laboratory, Chilton, Didcot,  
Oxon OX 10 QX, UK<sup>b</sup>

F. Barreiro, S. Brandt, M. Dittmar, M. Holder,  
G. Kreuzt, B. Neumann  
Fachbereich Physik der Universität-Gesamthochschule,  
D-5900 Siegen, Federal Republic of Germany<sup>a</sup>

E. Duchovni, Y. Eisenberg, U. Karshon,  
G. Mikenberg, R. Mir, D. Revel, A. Shapira  
Weizmann Institute, Rehovot, Israel<sup>c</sup>

G. Baranko, A. Caldwell, M. Cherney, J.M. Izen,  
M. Mermikides, S. Ritz, G. Rudolph<sup>6</sup>, D. Strom,  
M. Takashima, H. Venkataramania, E. Wicklund,  
Sau Lan Wu, G. Zobernig  
Department of Physics, University of Wisconsin, Madison,  
WI 53706, USA

Received 5 October 1984

1 On leave from Institute of Nuclear Physics, Cracow, Poland

2 On leave from Warsaw University, Poland

3 On leave from Weizmann Institute, Rehovot, Israel

4 Now at University of Glasgow, U.K.

5 Now at Institute of Oceanographic Sciences, Bidston, Merseyside, UK

6 Now at Inst. für Experimentalphysik der Universität Innsbruck

7 Now at University of Science and Technology of China, Hefei

8 On leave from Universiti Malaya, Kuala Lumpur

9 On leave from Rutherford Appleton Laboratory, Chilton, U.K.

<sup>a</sup> Supported by the Deutsches Bundesministerium für Forschung und Technologie

<sup>b</sup> Supported by the UK Science and Engineering Research Council

<sup>c</sup> Supported by the Minerva Gesellschaft für Forschung mbH

<sup>d</sup> Supported by the US Department of Energy contract DE-AC02-76 R 00881

**Abstract.** Results on  $K^0$  and  $\Lambda$  production in  $e^+e^-$  annihilation at c.m. energies of 14, 22 and 34 GeV are presented. The shape of the  $K^0$  and  $\Lambda$  differential cross sections are very similar to each other and to those of  $\pi^\pm$ ,  $K^\pm$  and  $p(\bar{p})$ . Scaling violations are observed for  $K^0$  production. We obtain a value for the probability to produce strange quark-antiquark pairs relative to that to produce up or down quark-antiquark pairs of  $0.35 \pm 0.02 \pm 0.05$ . The value of  $R_h = \sigma(e^+e^- \rightarrow hX)/\sigma_{\mu\mu}$  is shown to rise steadily with c.m. energy for all particle species. At 34 GeV we find  $1.48 \pm 0.05 K^0$  and  $0.31 \pm 0.03 \Lambda$  per event. We have searched for possible  $\Lambda$  polarization. The production of  $K^0$ 's and  $\Lambda$ 's in jets is examined as a function of  $p_T^2$  and rapidity and compared to that of all charged particles; the yields in two and three jets are also investigated. Results are presented from events with two baryons ( $\Lambda$ ,  $\bar{\Lambda}$ ,  $p$  or  $\bar{p}$ ) observed.

## 1. Introduction

Since the number of primary strange quarks is small in  $e^+e^-$  annihilation reactions compared to the number of strange particles produced, the latter will mostly result either from the decay of heavier quarks such as charm or bottom or from strange quark pairs produced during the fragmentation process. By studying the production of  $K^0$ 's and  $\Lambda$ 's\* we are able to study both the strange quark and baryon production mechanisms in the fragmentation of quarks to hadrons.

Results from this experiment on the total cross section and momentum distributions of  $K^0$ 's at centre of mass energies,  $W$ , of 30 and 33 GeV and of  $\Lambda$ 's at  $W=33$  GeV have been presented in previous publications [1, 2]. In this paper we present cross sections for  $K^0$  and  $\Lambda$  production at  $W=14, 22$  and 34 GeV. The improved statistics at  $W=34$  GeV allow a much more detailed study of  $K^0$  and  $\Lambda$  production than was possible previously. These results are complementary to our results on  $K^\pm$  and  $p, \bar{p}$  production in  $e^+e^-$  annihilation [3] and those from the TPC group at PEP [4]. Data on high energy  $K^0$  and  $\Lambda$  production have also been reported in [5, 6] and [7].

## 2. Analysis

The experiment was performed at the  $e^+e^-$  storage ring PETRA using the TASSO detector. The analy-

\* The term  $K^0$  will be used to refer to both  $K^0$  and  $\bar{K}^0$  and  $\Lambda$  to refer to both  $\Lambda$  and  $\bar{\Lambda}$

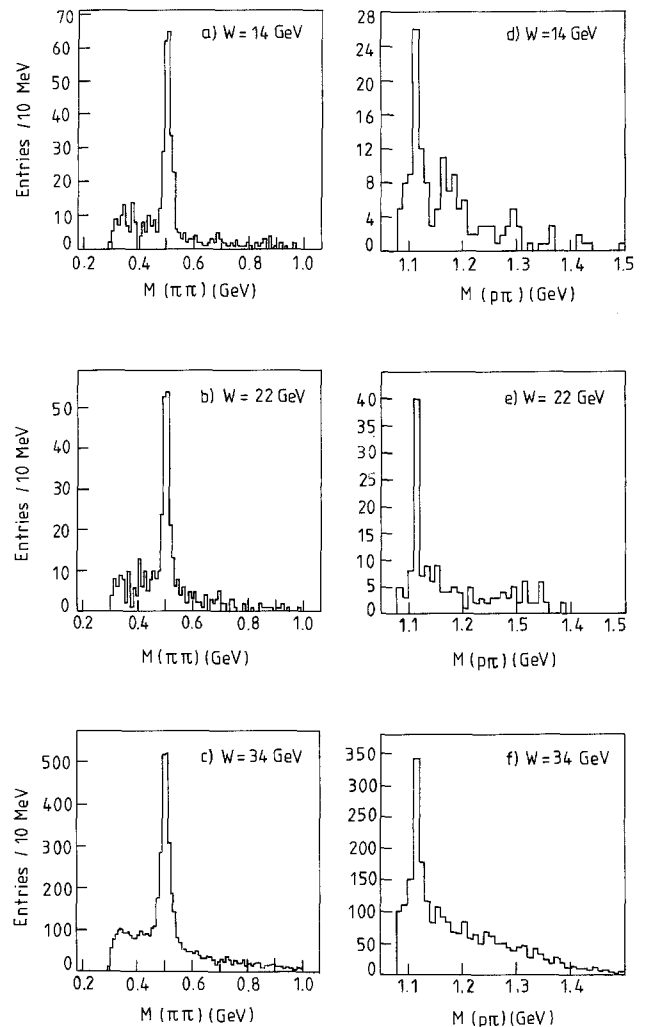


**Fig. 1 a-f.**  $\pi^+\pi^-$  and  $p\pi^-$  ( $\bar{p}\pi^+$ ) effective mass distributions after the cuts to select the basic  $K^0$  and  $\Lambda$  samples. The  $K^0$  plots at 14, 22 and 34 GeV are shown in a, b and c; the corresponding  $\Lambda$  plots in d, e and f

sis procedures for selecting hadronic annihilation events have been described elsewhere [8]. A total of 2,705, 1,889 and 20,832 hadronic events were used in this analysis at  $W=14, 22$  and 34 GeV. The 34 GeV data were taken between  $W=30$  and 36.7 GeV with an average value of 34.4 GeV. The cuts used to obtain the  $K^0$  and  $\Lambda$  samples are essentially as described in Refs. 1 and 2; they do not use any particle identification and as a result for the  $\Lambda$ 's we imposed a minimum momentum cut of 1 GeV/c to obtain a satisfactory signal to background ratio. The invariant mass of all  $\pi^+\pi^-$  and  $p\pi^-$  ( $\bar{p}\pi^+$ ) combinations satisfying these cuts is shown in Fig. 1 for the three c.m. energies. The  $K^0$  and  $\Lambda$  mass distributions integrated over all momenta have standard deviations of 18 MeV and 7 MeV respectively. The numbers of  $K_s^0 \rightarrow \pi^+\pi^-$  candidates in the range 0.45

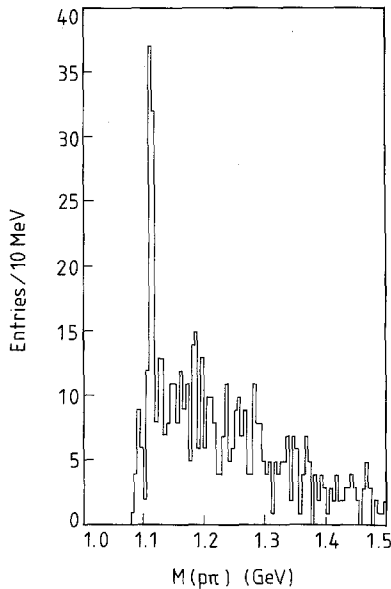


**Fig. 2.** The  $p\pi^-$  ( $\bar{p}\pi^+$ ) mass spectrum at  $W=34$  GeV obtained using the time of flight counters to identify low momentum protons and antiprotons

to 0.55 GeV satisfying the cuts were 200, 145 and 1,708 over backgrounds of 50, 62 and 729 at  $W=14$ , 22 and 34 GeV. The corresponding numbers of  $\Lambda \rightarrow p\pi^-$  (or  $\bar{\Lambda} \rightarrow \bar{p}\pi^+$ ) candidates in the range 1.10 to 1.13 GeV were 28, 38 and 385 over backgrounds of 19, 15 and 285. Approximately equal numbers of  $\Lambda$ 's and  $\bar{\Lambda}$ 's were observed; the numbers of  $\Lambda$ 's were 12, 22 and 196 at the three energies compared with 16, 16 and 189 for  $\bar{\Lambda}$ 's.

The  $\Lambda$  cross section below 1 GeV/c was obtained in the following way. Information from the Inner Time of Flight counters [3] was used to enhance the fraction of low momentum protons and antiprotons, and extend the  $\Lambda$  momentum range down to 0.6 GeV/c. A track was accepted as a proton provided that the measured time was within 3 standard deviations of that expected for a proton. It was not accepted if the time was within 0.5 standard deviations of that expected for a kaon or within one standard deviation of that expected for a pion. Figure 2 shows the  $p\pi^-$  ( $\bar{p}\pi^+$ ) invariant mass combinations with momenta between 0.6 and 1.5 GeV/c obtained using the time of flight information. In the mass range from 1.10 to 1.13 GeV there are 60  $\Lambda$ 's over a background of 21.

The efficiency for a  $K^0$  or  $\Lambda$  to be found by the pattern recognition programs and to survive the cuts was estimated by a Monte Carlo program which simulated hits in the tracking chambers as well as decays, nuclear absorption and scattering. The simulated events were then subjected to the same chain of analysis programs as the real data. The efficiency

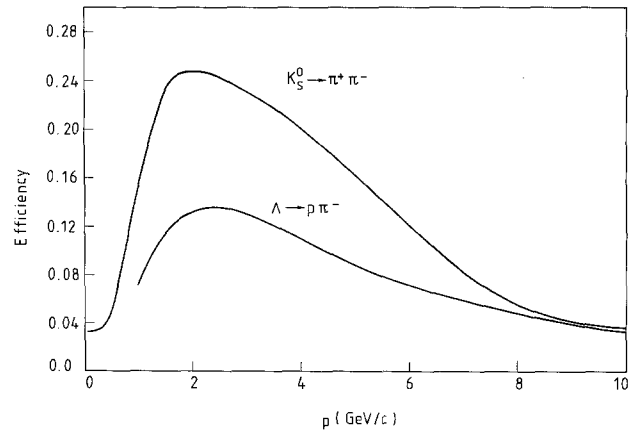


**Fig. 3.** The efficiency as a function of momentum for detecting the decays  $K_s^0 \rightarrow \pi^+\pi^-$  and  $\Lambda \rightarrow p\pi^-$  ( $\bar{\Lambda} \rightarrow \bar{p}\pi^+$ ) at  $W=34$  GeV

calculations include the effects of initial state radiation. The efficiency for detection of  $K_s^0 \rightarrow \pi^+\pi^-$  and  $\Lambda \rightarrow p\pi^-$  at  $W=34$  GeV by the first method described above is shown in Fig. 3. In addition the data were corrected for unseen decay channels and for  $K_L^0$  production.

To calculate the  $\Lambda$  cross section between 0.6 and 1.0 GeV/c, where the time of flight counters were used, Monte Carlo simulation was used to obtain the relative efficiency in the ranges 0.6–1.0 GeV/c and 1.0–1.5 GeV/c. The overall efficiency was then obtained by setting the cross section from this second method between 1.0 and 1.5 GeV/c equal to that obtained by the first method.

The systematic error on the cross sections arises from uncertainties in the efficiency of the track finding, the effects of absorption in the detector materials, the estimation of background, the effects of the cuts and the value of the total cross section [8]. These uncertainties have been estimated by making detailed studies of the drift chamber and track finding efficiencies, by repeating the efficiency calculations using different Monte Carlo programs and by varying the cuts. We estimate that the overall normalization error on the cross sections presented below is 15% for  $K^0$ 's and 20% for  $\Lambda$ 's. Approximately half of this error is independent of  $W$ .

### 3. Differential Cross Sections

Figure 4 and Table 1 show the scaled cross sections  $s/\beta d\sigma/dx$  for  $K^0$  and  $\Lambda$  production at  $W=14$ , 22 and 34 GeV, where  $s=W^2$ ,  $\beta=p/E$  and  $x=2E/W$ ;  $p$  is the particle's momentum and  $E$  its energy. The corresponding differential cross sections  $d\sigma/dp$  are given in Table 2. The data are in agreement with our

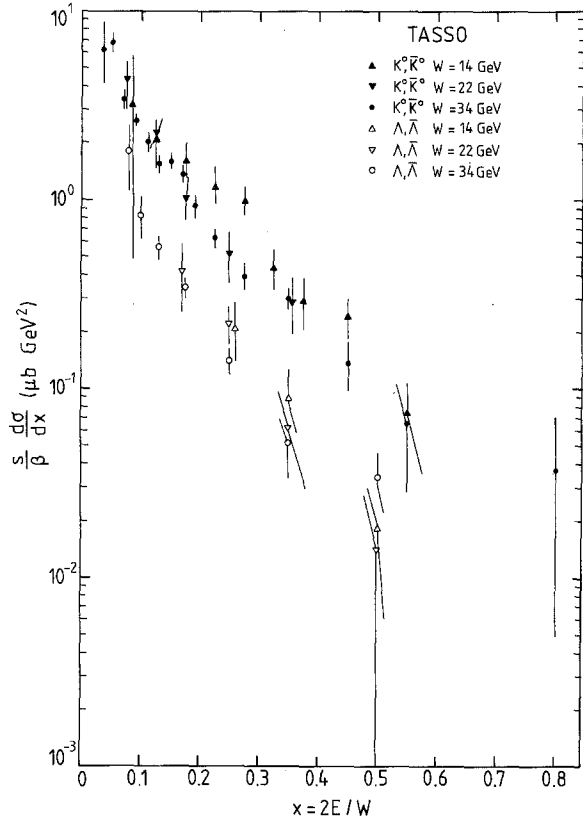


**Fig. 4.** The scaled cross section  $s/\beta d\sigma/dx$  as a function of  $x$  for  $K^0$ ,  $\bar{K}^0$  and  $\Lambda$ ,  $\bar{\Lambda}$  production at  $W=14$ , 22 and 34 GeV

previous measurements at 33 GeV [1, 2], with  $K^0$  results from JADE [5] and PLUTO [6] and with  $\Lambda$  results from JADE [7]. The  $K^0$  data show scaling violation for  $x > 0.2$ . In this range the 14 GeV data lie systematically above the high energy data, the  $K^0$  scaled cross section being reduced by  $49 \pm 7 \pm 5\%$  on average from  $W=14$  GeV to  $W=34$  GeV. Given the larger errors on the  $\Lambda$  cross sections it is not possible to draw a definite conclusion on scaling for  $\Lambda$  production. The data for  $x > 0.2$  show a  $34 \pm 19 \pm 6\%$  reduction in the scaled cross section between  $W=14$  and  $W=34$  GeV. These results can be compared with the scaling violations observed in charged particle production [5, 9, 10] where there is a  $\sim 20\%$  reduction in the scaled cross section over the same kinematic range.

Figure 5 shows the scaled cross section  $s/\beta d\sigma/dx$  for  $K^0$ 's and  $\Lambda$ 's at  $W=34$  GeV together with results on  $\pi^\pm$ ,  $K^\pm$ ,  $p(\bar{p})$  and  $\Xi^-(\bar{\Xi}^-)$  production measured in this experiment [3, 11]. All particle species show approximately the same  $x$  dependence suggesting a similar production mechanism for all strange and non-strange hadrons. The  $K^0$  data lie systematically below the  $K^\pm$  data by  $\sim 25\%$  which is outside the

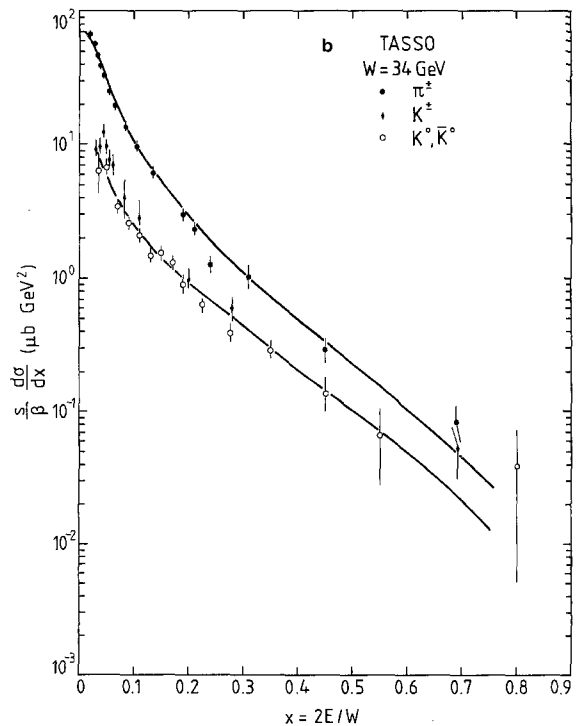
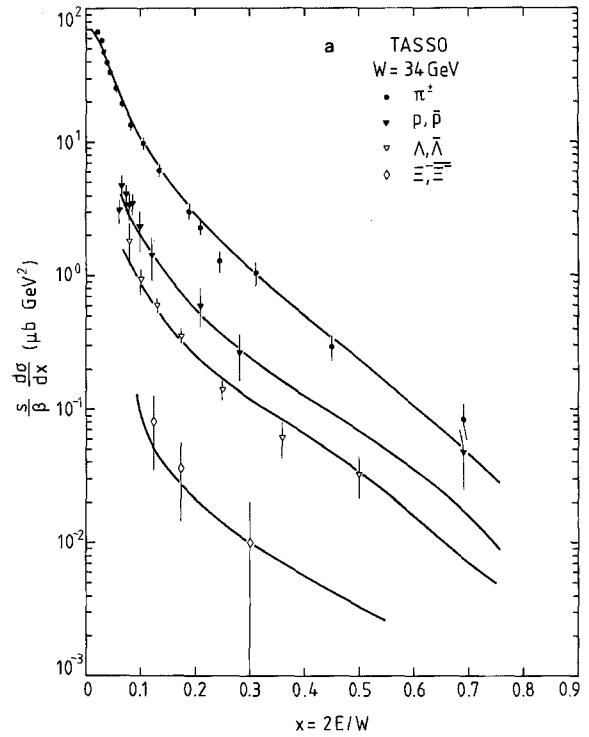


**Fig. 5a and b.** The scaled cross section  $s/\beta d\sigma/dx$  as a function of  $x$  for **a**  $\pi^\pm$ ,  $p$ ,  $\bar{p}$ ,  $\Lambda$ ,  $\bar{\Lambda}$  and  $\Xi^-$ ,  $\bar{\Xi}^-$ , **b**  $\pi^\pm$ ,  $K^\pm$  and  $K^0$ ,  $\bar{K}^0$  at  $W=34$  GeV. The curves are fits using the Lund model with the parameters as described in the text

**Table 1.** The scaled cross section  $s/\beta d\sigma/dx$  ( $\mu\text{b}\cdot\text{GeV}^2$ ) for  $K^0$ ,  $\bar{K}^0$  and  $\Lambda$ ,  $\bar{\Lambda}$  production at  $W=14, 22$  and  $34$  GeV  
**a**  $K^0, \bar{K}^0$

$W=14$ GeV		$W=22$ GeV		$W=34$ GeV	
$x$	$s/\beta d\sigma/dx$	$x$	$s/\beta d\sigma/dx$	$x$	$s/\beta d\sigma/dx$
0.07–0.10	$3.16 \pm 2.68$	0.05–0.10	$4.26 \pm 1.18$	0.03–0.04	$6.41 \pm 2.33$
0.10–0.15	$2.10 \pm 0.63$	0.10–0.15	$2.27 \pm 0.41$	0.04–0.06	$6.79 \pm 0.77$
0.15–0.20	$1.61 \pm 0.31$	0.15–0.20	$1.04 \pm 0.51$	0.06–0.08	$3.34 \pm 0.35$
0.20–0.25	$1.17 \pm 0.22$	0.20–0.30	$0.51 \pm 0.14$	0.08–0.10	$2.63 \pm 0.24$
0.25–0.30	$0.98 \pm 0.17$	0.30–0.40	$0.29 \pm 0.10$	0.10–0.12	$2.08 \pm 0.19$
0.30–0.35	$0.44 \pm 0.12$	0.40–0.50	$0.05 \pm 0.07$	0.12–0.14	$1.54 \pm 0.15$
0.35–0.40	$0.29 \pm 0.09$			0.14–0.16	$1.59 \pm 0.15$
0.40–0.50	$0.24 \pm 0.06$			0.16–0.18	$1.35 \pm 0.15$
0.50–0.60	$0.07 \pm 0.04$			0.18–0.20	$0.91 \pm 0.12$
				0.20–0.25	$0.63 \pm 0.07$
				0.25–0.30	$0.39 \pm 0.06$
				0.30–0.40	$0.30 \pm 0.04$
				0.40–0.50	$0.14 \pm 0.04$
				0.50–0.60	$0.068 \pm 0.040$
				0.60–1.00	$0.038 \pm 0.037$

**b**  $\Lambda, \bar{\Lambda}$

$W=14$ GeV		$W=22$ GeV		$W=34$ GeV	
$x$	$s/\beta d\sigma/dx$	$x$	$s/\beta d\sigma/dx$	$x$	$s/\beta d\sigma/dx$
0.22–0.30	$0.21 \pm 0.07$	0.14–0.20	$0.42 \pm 0.17$	0.075–0.09	$1.84 \pm 0.72$
0.30–0.40	$0.089 \pm 0.032$	0.20–0.30	$0.22 \pm 0.05$	0.09–0.11	$0.82 \pm 0.19$
0.40–0.60	$0.018 \pm 0.012$	0.30–0.40	$0.062 \pm 0.033$	0.11–0.15	$0.56 \pm 0.07$
		0.40–0.60	$0.014 \pm 0.013$	0.15–0.20	$0.34 \pm 0.04$
				0.20–0.30	$0.14 \pm 0.02$
				0.30–0.40	$0.060 \pm 0.018$
				0.40–0.60	$0.032 \pm 0.015$

systematic errors of the two measurements. No experimental effect has been found to explain this difference. We have checked that consistent results are obtained for  $K^0$ 's that decay before and after the beam pipe and have repeated the analysis of low momentum ( $<1$  GeV/c) data without any cuts. Small differences could possibly result from charm decays,  $\phi$  meson decays and the predominance of leading  $u$  quarks over leading  $d$  quarks, however all these effects are included in our Monte Carlo programs which predict almost equal numbers of  $K^\pm$  and  $K^0$ .

Assuming that the fragmentation of quarks into hadrons proceeds via the production of quark-antiquark and diquark-antiquark pairs one can use these particle spectra to estimate the relative proportions of strange and non-strange quarks and diquarks in the fragmentation process.

After adjustment of fragmentation parameters the Lund Monte Carlo program [12, 13] provides a reasonable description of the overall features of hadron production in  $e^+e^-$  annihilation such as the

charged particle multiplicity and  $x$  distributions. In this program, the relative amounts of pion, kaon, proton, lambda and cascade production are primarily controlled by three parameters; the ratio of strange quarks to non-strange quarks,  $P(s)/P(u)$  ( $=P(s)/P(d)$ ), the ratio of diquark pair to quark pair production  $P(qq)/P(q)$ , and the extra suppression of strangeness in diquark pairs

$$d = \frac{P(us)/P(ud)}{P(s)/P(d)}.$$

From the ratio of the proton to pion cross sections we obtain  $P(qq)/P(q) = 0.10 \pm 0.01$  independent of the value of the other two parameters. Fixing  $P(qq)/P(q) = 0.10$  the ratio of the  $K^0$  to pion cross sections yields  $P(s)/P(u) = 0.35 \pm 0.02 \pm 0.05^*$  independent of the value of  $d$ . This result can be compared with the value of  $0.27 \pm 0.03 \pm 0.05$  obtained by JADE [5]. With  $P(qq)/P(q) = 0.10$  and  $P(s)/P(u) = 0.35$  the ratio

\* Using our previous  $K^\pm$  measurements we would obtain  $P(s)/P(u) = 0.58 \pm 0.04 \pm 0.07$

**Table 2.** The differential cross section  $d\sigma/dp$  (nb/GeV/c) for  $K^0$ ,  $\bar{K}^0$  and  $\Lambda$ ,  $\bar{\Lambda}$  production at  $W=14, 22$  and  $34$  GeV**a**  $K^0, \bar{K}^0$ 

$W=14$ GeV		$W=22$ GeV		$W=34$ GeV	
$p$	$d\sigma/dp$	$p$	$d\sigma/dp$	$p$	$d\sigma/dp$
0.00–0.50	$0.88 \pm 0.65$	0.00– 0.50	$0.21 \pm 0.33$	0.00– 0.25	$0.044 \pm 0.023$
0.50–0.75	$0.84 \pm 0.42$	0.50– 1.00	$0.51 \pm 0.13$	0.25– 0.50	$0.123 \pm 0.037$
0.75–1.00	$1.02 \pm 0.27$	1.00– 1.20	$0.46 \pm 0.13$	0.50– 0.75	$0.205 \pm 0.038$
1.00–1.20	$0.92 \pm 0.27$	1.20– 1.40	$0.31 \pm 0.11$	0.75– 1.00	$0.170 \pm 0.022$
1.20–1.40	$0.93 \pm 0.22$	1.40– 1.60	$0.33 \pm 0.09$	1.00– 1.20	$0.135 \pm 0.020$
1.40–1.60	$0.66 \pm 0.19$	1.60– 1.80	$0.22 \pm 0.08$	1.20– 1.40	$0.131 \pm 0.016$
1.60–1.80	$0.70 \pm 0.15$	1.80– 2.00	$0.16 \pm 0.07$	1.40– 1.60	$0.119 \pm 0.013$
1.80–2.00	$0.56 \pm 0.14$	2.00– 2.50	$0.095 \pm 0.043$	1.60– 1.80	$0.091 \pm 0.012$
2.00–2.50	$0.33 \pm 0.07$	2.50– 3.00	$0.081 \pm 0.038$	1.80– 2.00	$0.095 \pm 0.012$
2.50–3.00	$0.19 \pm 0.05$	3.00– 4.00	$0.077 \pm 0.021$	2.00– 2.50	$0.074 \pm 0.006$
3.00–4.00	$0.10 \pm 0.03$	4.00– 6.00	$0.014 \pm 0.009$	2.50– 3.00	$0.066 \pm 0.006$
4.00–7.00	$0.005 \pm 0.005$	6.00–11.00	$0.000 \pm 0.005$	3.00– 3.50	$0.046 \pm 0.005$
				3.50– 4.00	$0.028 \pm 0.004$
				4.00– 5.00	$0.022 \pm 0.003$
				5.00– 6.00	$0.018 \pm 0.003$
				6.00– 7.00	$0.013 \pm 0.003$
				7.00– 8.00	$0.0077 \pm 0.0028$
				8.00–10.00	$0.0028 \pm 0.0021$
				10.00–12.00	$0.0015 \pm 0.0012$
				12.00–17.00	$0.0023 \pm 0.0023$

**b**  $\Lambda, \bar{\Lambda}$ 

$W=14$ GeV		$W=22$ GeV		$W=34$ GeV	
$p$	$d\sigma/dp$	$p$	$d\sigma/dp$	$p$	$d\sigma/dp$
1.0–2.0	$0.089 \pm 0.034$	1.0–2.0	$0.052 \pm 0.014$	0.6– 1.0	$0.033 \pm 0.013$
2.0–4.0	$0.021 \pm 0.008$	2.0–3.0	$0.032 \pm 0.010$	1.0– 1.5	$0.025 \pm 0.006$
		3.0–5.0	$0.010 \pm 0.004$	1.5– 2.0	$0.022 \pm 0.004$
				2.0– 3.0	$0.017 \pm 0.002$
				3.0– 4.0	$0.0081 \pm 0.0015$
				4.0– 5.0	$0.0061 \pm 0.0012$
				5.0– 7.0	$0.0031 \pm 0.0009$
				7.0–10.0	$0.0017 \pm 0.0008$

of the lambda to proton cross sections gives  $d=0.26 \pm 0.07$ , in agreement with that obtained from the ratio of cascade to proton cross sections  $d=0.32 \pm 0.13$ . The curves on Fig. 5 show the predictions of the Lund Monte Carlo using  $P(qq)/P(q)=0.10$ ,  $P(s)/P(u)=0.35$  and  $d=0.32$ .

#### 4. Integrated Cross Sections

The total inclusive cross sections relative to  $\sigma_{\mu\mu} = 4\pi\alpha^2/3s$

$$R_h = \frac{\sigma(e^+ e^- \rightarrow hX) + \sigma(e^+ e^- \rightarrow \bar{h}X)}{\sigma_{\mu\mu}}$$

where  $h=K^0$  or  $\Lambda$ , were obtained by integrating the differential cross sections. In the  $K^0$  case the cross

section was measured over the full momentum range. In the  $\Lambda$  case unmeasured contributions from the low momentum ( $p < 1.0, 1.0, 0.6$  GeV/c at  $W = 14, 22, 34$  GeV) and very high momentum ( $p > 4.0, 5.0, 10.0$  GeV/c) regions have been estimated using the Lund Monte Carlo. The unmeasured contribution amounts to 43%, 35% and 14% at  $W=14, 22$  and  $34$  GeV. The systematic error on  $R_h$  includes a contribution due to the uncertainty in this estimation. The  $R_h$  values are given in Table 3 and plotted in Fig. 6 along with low energy data from PLUTO [14], SLAC-LBL [15, 16] and DASP [17, 18] and high energy data from JADE [5] and this experiment [3]. The higher mass particles show a somewhat steeper rise of  $R_h$  with increasing  $W$ . The multiplicity of each particle species at  $W=14, 22$  and  $34$  GeV as measured in this experiment is given in Table 4. In this table the numbers include all

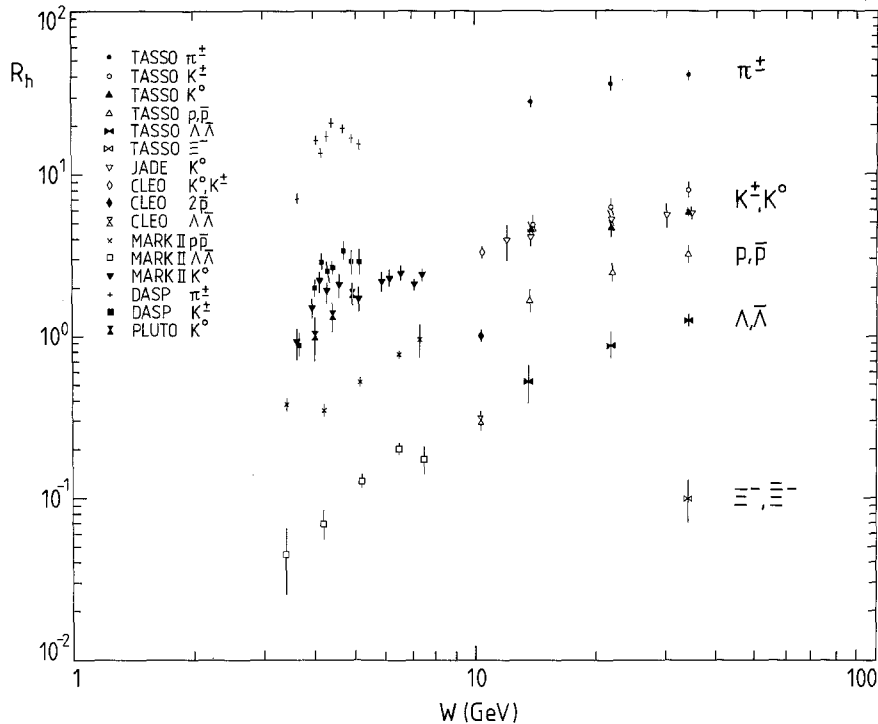


**Fig. 6.** The total cross section  $R_h = \sigma(e^+e^- \rightarrow hX) + \sigma(e^+e^- \rightarrow \bar{h}X) / \sigma_{\mu\mu}$  as a function of  $W$  for  $\pi^\pm$ ,  $K^\pm$ ,  $K^0$ ,  $\bar{K}^0$ ,  $\rho$ ,  $\bar{p}$ ,  $A$ ,  $\bar{A}$  and  $\Xi^-$ ,  $\bar{\Xi}^-$

**Table 3.** The total cross section for  $K^0$ ,  $\bar{K}^0$  and  $A$ ,  $\bar{A}$  production  $R_h = \frac{\sigma(e^+e^- \rightarrow hX) + \sigma(e^+e^- \rightarrow \bar{h}X)}{\sigma_{\mu\mu}}$ . The first error is statistical the second systematic

$W$ (GeV)	$R_{K^0}$	$R_A$
14	$4.59 \pm 0.40 \pm 0.69$	$0.53 \pm 0.14 \pm 0.12$
22	$4.66 \pm 0.53 \pm 0.70$	$0.89 \pm 0.18 \pm 0.19$
34	$5.92 \pm 0.20 \pm 0.89$	$1.26 \pm 0.11 \pm 0.25$

**Table 4.** Particle multiplicity per event measured by TASSO

	$W=14$ GeV	$W=22$ GeV	$W=34$ GeV
$\pi^\pm$	$7.2 \pm 0.6$	$8.8 \pm 1.0$	$10.3 \pm 0.4$
$K^\pm$	$1.2 \pm 0.14$	$1.5 \pm 0.2$	$2.0 \pm 0.2$
$K^0, \bar{K}^0$	$1.15 \pm 0.10$	$1.17 \pm 0.13$	$1.48 \pm 0.05$
$\rho^0$	-	-	$0.73 \pm 0.06$
$p, \bar{p}$	$0.42 \pm 0.06$	$0.62 \pm 0.06$	$0.80 \pm 0.10$
$A, \bar{A}$	$0.13 \pm 0.04$	$0.22 \pm 0.05$	$0.31 \pm 0.03$
$\Xi^-, \bar{\Xi}^-$	-	-	$0.026 \pm 0.008$

decay products from particles with lifetimes less than  $3.10^{-10}$  s. For example the number of pions includes those from  $\rho$ ,  $K_s^0$ ,  $A$  decay etc.

### 5. Lambda Polarization

The weak decay of the  $\Lambda$  enables a measurement to be made of its polarization from the decay asym-

metry with respect to some axis. We first discuss this on the assumption that the annihilation process is purely a first order parity conserving e.m. process.

For the longitudinal polarization the  $A$  direction in the laboratory system was the chosen axis and the forward backward asymmetry of the decay proton in the  $A$  rest frame was measured. The asymmetry is defined as

$$A_L = \frac{N_f - N_b}{N_f + N_b}$$

where  $N_f(N_b)$  are the number of  $\Lambda$ 's with the decay proton in the forward (backward) hemisphere defined by the  $A$  direction in the laboratory. After correction for losses due to the  $\Lambda$  selection procedure, this asymmetry is related to the longitudinal polarization  $P_L$  by

$$P_L = \frac{2}{\alpha} A_L$$

where  $\alpha=0.642$  is the  $\Lambda$  decay parameter. Parity conservation in the production process demands that primary particles show no longitudinal polarization and therefore any such  $\Lambda$  polarization must result from the  $\Lambda$ 's being decay products of weakly decaying heavier states such as  $\Lambda_c$  etc. CP conservation in such a decay demands that  $\Lambda$ 's and  $\bar{\Lambda}$ 's should show opposite polarization. The same con-

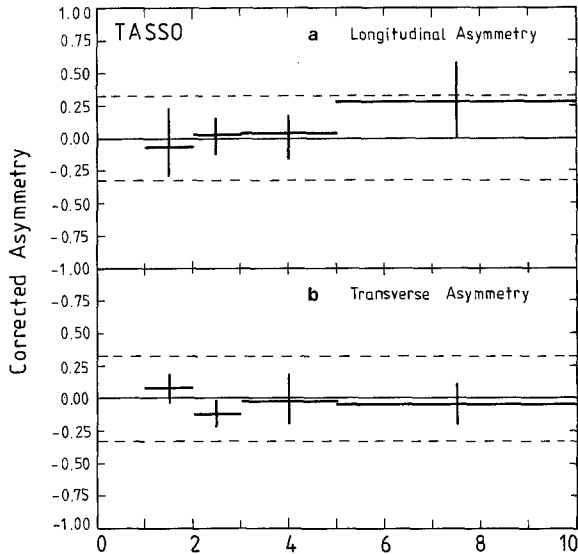


**Fig. 7 a and b.** The decay asymmetries **a** longitudinal and **b** transverse for  $\Lambda$  and  $\bar{\Lambda}$  as a function of momentum. The dashed lines indicate the asymmetry that would be obtained for 100% polarization

siderations require that the resulting asymmetry from  $\Lambda$  and  $\bar{\Lambda}$  decays of opposite longitudinal polarization must be the same. The decay asymmetry is shown in Fig. 7a for  $\Lambda$  and  $\bar{\Lambda}$  together as a function of momentum. Within errors no significant asymmetry or trend with momentum is observed and hence there is no evidence for any longitudinal polarization of the  $\Lambda$ 's. In the region from 2 to 5 GeV/c where the  $\Lambda$  signal is cleanest, the average asymmetry is  $+0.02 \pm 0.10$  and we obtain longitudinal polarization values of  $-0.12 \pm 0.44$  for the  $\Lambda$ 's and  $-0.19 \pm 0.45$  for the  $\bar{\Lambda}$ 's.

Measurement of a longitudinal  $\Lambda$  polarization has been proposed as a method for measuring the polarization of the primary quarks resulting from  $Z^0$  exchange and  $\gamma-Z^0$  interference [19, 20]. As the c.m. energy approaches the  $Z^0$  mass this becomes large even with unpolarised incident beams and such a measurement would provide a valuable test of the standard model. However, at our energy the values predicted by the standard model for both  $Q = +2/3$  and  $Q = -1/3$  quarks, integrated over all production angles is less than 0.1. The resultant  $\Lambda$  polarization depends upon the details of the fragmentation process but will be even less. Consequently with our present statistics at this energy we are insensitive to such effects.

A transverse polarization of the primary particles conserves parity in the annihilation process. For the  $\Lambda$ 's this was searched for by examination of the angular distribution of the decay proton in the  $\Lambda$  rest frame with respect to the normal to the  $\Lambda$

production plane. We define

$$\text{Cos}\theta_T = \frac{\mathbf{p} \cdot (\mathbf{e}^+ \times \mathbf{A})}{|\mathbf{p}| |\mathbf{e}^+ \times \mathbf{A}|}$$

where  $\mathbf{p}$  is the momentum of the  $p(\bar{p})$  in the  $\Lambda(\bar{\Lambda})$  rest frame,  $\mathbf{e}^+$  is the momentum of the  $e^+$  beam in the laboratory and  $\mathbf{A}$  is the momentum of the  $\Lambda(\bar{\Lambda})$  in the laboratory.

The asymmetry is defined by

$$A_T = \frac{N_{\text{up}} - N_{\text{down}}}{N_{\text{up}} + N_{\text{down}}}$$

where  $N_{\text{up}}$  and  $N_{\text{down}}$  are the number of decays with  $0.0 < \text{Cos}\theta_T < 1.0$  and  $-1.0 < \text{Cos}\theta_T < 0.0$  respectively. After efficiency corrections this is related to the transverse  $\Lambda$  polarization by

$$P_T = \frac{2}{\alpha} A_T.$$

With the above definitions  $C$  conservation and the forward-backward symmetry of the lowest order annihilation process require that the asymmetry will be the same for  $\Lambda$  and  $\bar{\Lambda}$  at a particular production angle. Hence, again,  $\Lambda$  and  $\bar{\Lambda}$  were combined to search for any possible asymmetry. This asymmetry is plotted against momentum in Fig. 7b. No evidence for any non-zero value is observed. Between 2 and 5 GeV/c the average asymmetry is  $0.07 \pm 0.08$  and we obtain a value for the transverse polarization of  $\Lambda$ 's of  $-0.33 \pm 0.33$  and for  $\bar{\Lambda}$ 's of  $+0.31 \pm 0.32$ .

## 6. $K^0$ and $\Lambda$ Production in Jets

We have investigated the production of  $K^0$ 's and  $\Lambda$ 's in jets produced in  $e^+e^-$  annihilation at  $W=34$  GeV. We first analyse all events as two jet events. Figure 8a shows the production cross sections for  $K^0$ 's and  $\Lambda$ 's normalized to the total cross section as a function of the folded rapidity  $y = \frac{1}{2} \ln \frac{E + |p_L|}{E - |p_L|}$ , where  $p_L$  is the momentum component parallel to the thrust axis of the event. Also plotted is the same distribution for all charged particles assuming them to be pions. The data are corrected for acceptance, efficiency and initial state radiation. The distribution for  $K^0$ 's has a similar plateau to that for the charged particles. The shape of the plateau region in the  $\Lambda$  case is harder to establish since there is no reliable data for  $y < 0.5$  due to the difficulty of reconstructing very low momentum  $\Lambda$ 's. In Fig. 8b we show the same distributions plotted as a function of  $y - y_{\text{max}}$  where  $y_{\text{max}}$  is the maximum possible rapidity given

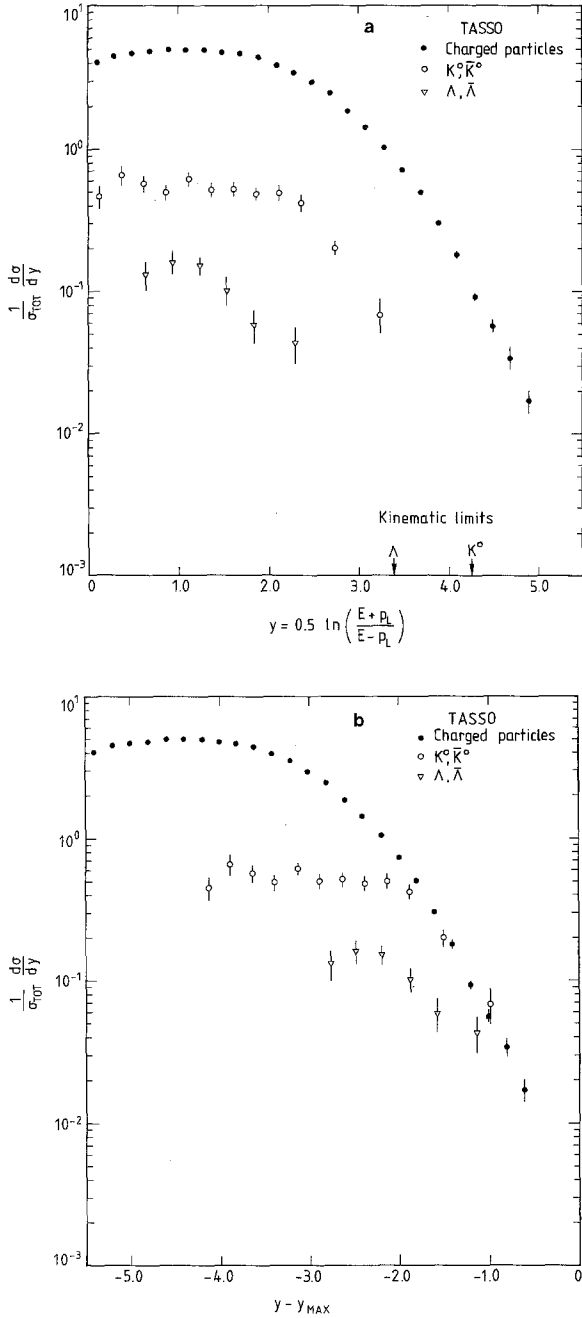


**Fig. 8a and b.** The differential cross section for  $K^0$ ,  $\bar{K}^0$ ,  $\Lambda$ ,  $\bar{\Lambda}$  and charged particle production normalized to the total hadronic cross section **a** as a function of rapidity  $y$  and **b** as a function of  $y - y_{\max}$

by  $y_{\max} \sim \ln(W/M)$  and  $M$  is the particle mass. For  $y - y_{\max} > -2.0$  the  $K^0$  and the charged particle data lie on the same curve. The  $\Lambda$  data however fall below this curve.

In Fig. 9 we show the corrected  $d\sigma/dp_T^2$  distributions for  $K^0$ 's,  $\Lambda$ 's and all charged particles at  $W = 34$  GeV, where  $p_T$  is the momentum component transverse to the sphericity axis of the event. At low

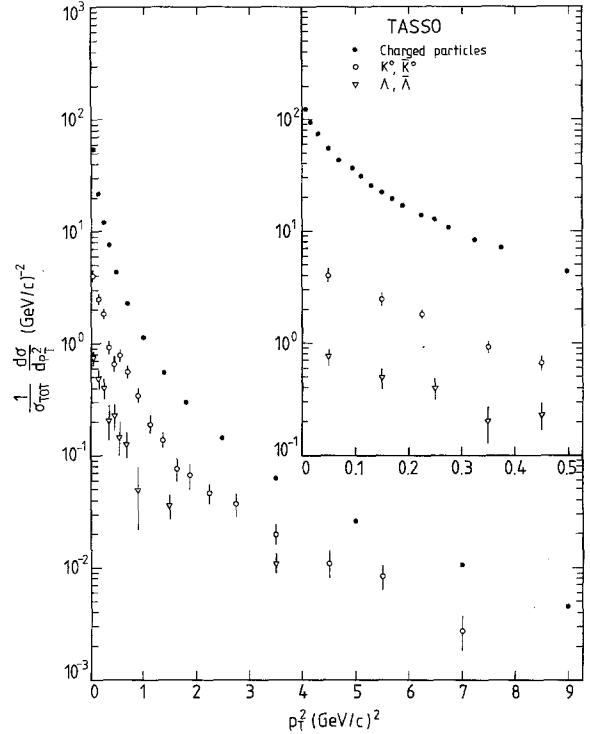


**Fig. 9.** The differential cross section for  $K^0$ ,  $\bar{K}^0$ ,  $\Lambda$ ,  $\bar{\Lambda}$  and charged particle production normalized to the total hadronic cross section as a function of  $p_T^2$ . The insert shows the region  $p_T^2 < 0.5$  in more detail

$p_T^2 (< 0.5 \text{ (GeV/c)}^2)$  the  $K^0$  and  $\Lambda$  distributions can be described by  $Ae^{(-p_T^2/2\sigma^2)}$  with  $\sigma = 0.31 \pm 0.01$  GeV/c for  $K^0$ 's and  $\sigma = 0.38 \pm 0.04$  GeV/c for  $\Lambda$ 's. For charged particles the distribution rises sharply for very low  $p_T^2$  values. This probably reflects the fact that most of these particles are pions from the decay of heavier particles where the  $p_T^2$  of the parent is shared between several decay products. In contrast a large proportion of the  $K^0$ 's and  $\Lambda$ 's are expected to be directly produced in the fragmentation process.

All three distributions show a long tail at high  $p_T^2$  as expected from QCD. This indicates that  $K^0$ 's and  $\Lambda$ 's are produced both in two and three jet events.

We compared the yield of  $K^0$ 's and  $\Lambda$ 's in two and three jet events in the following manner. The method of generalized sphericity [21] was used to resolve each event into three separate jets and to find the three jet axes. From the angles between the three jets the fractional energies  $x_i$  of the jets were calculated assuming massless partons and demanding that  $\sum x_i = 2$ . Events were considered as three jet events if all the jets in the event had  $x_i < 0.9$  and  $\sum |p_j| > 1.5$  GeV/c where  $p_j$  are the momenta of the charged tracks in the jet. In order to suppress events with initial state hard photon radiation the angle

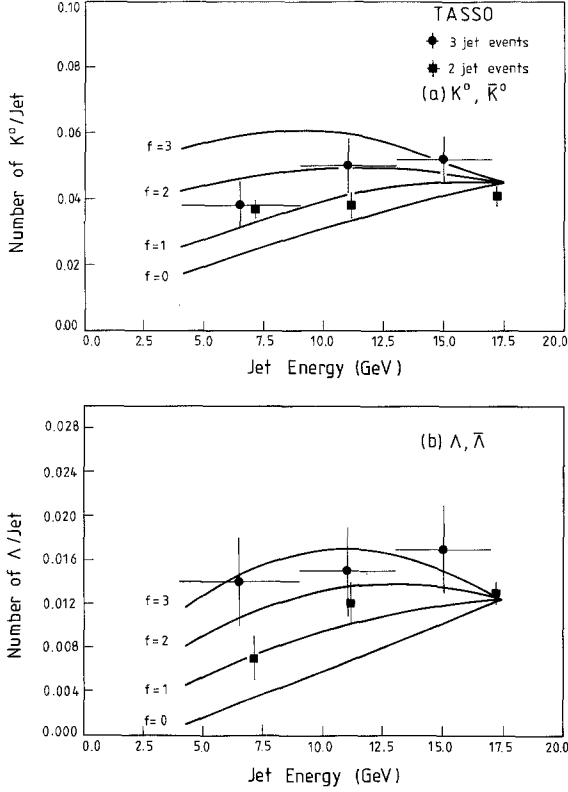


**Fig. 10a and b.** The observed yield of **a**  $K^0$ 's and **b**  $\Lambda$ 's as a function of jet energy in two jet events at  $W=14, 22$  and  $34$  GeV and three jet events at  $W=34$  GeV. The curves represent Monte Carlo predictions for the three jet events assuming the  $K^0$  or  $\Lambda$  content of gluon jets is  $f$  times that of quark jets for  $f$  values of 0, 1, 2 and 3

between the normal to the event plane and the beam axis was required to be less than  $70^\circ$ . A total of 1,402 events at  $W=34$  GeV passed these criteria. The  $K^0$ 's and  $\Lambda$ 's were then associated with the jet whose axis was closest to the  $K^0/\Lambda$  momentum vector. Figures 10a and b show the *observed*  $K^0$  and  $\Lambda$  yields per jet as a function of jet energy, where the jet energy is given by the fractional energy,  $x_i$ , times the beam energy. Also plotted are the observed  $K^0$  and  $\Lambda$  yields per jet in two jet events at  $W=14, 22$  and  $34$  GeV. In this case all events were treated as two jet events and the jet energy was assumed to be the beam energy. The efficiency for finding  $K^0$ 's and  $\Lambda$ 's at a given jet energy was found to be the same within 20% independent of whether the jet was from a two or three jet event. If there were a large increase in the  $K^0$  or  $\Lambda$  yield in jets associated with gluons one would expect an increased yield in the three jet events particularly for the lower jet energy. To illustrate this we generated Monte Carlo events in which we varied the relative amount,  $f$ , of  $K^0$  and  $\Lambda$  production in the gluon jet to that in the quark jet. Predictions for the observed  $K^0$  and  $\Lambda$  yields in

the three jet events for  $f=0, 1, 2$  and 3 are shown in Fig. 10.

We note that on the  $T$  resonance which dominantly decays to three gluons, there is a threefold increase in the  $\Lambda/K$  ratio over the adjacent  $q\bar{q}$  continuum [22]. Whilst our results shown in Fig. 10 are consistent with this the large errors on our three jet data points prevent us drawing any definite conclusions.

## 7. $\Lambda$ Correlations

We looked for correlations between the  $\Lambda(\bar{\Lambda})$  and other particles in the event which compensated either the baryon number or strangeness of the  $\Lambda(\bar{\Lambda})$ . A sample of 246  $\Lambda$  or  $\bar{\Lambda}$  candidates above a background of 73 was obtained by demanding that the  $\Lambda$  or  $\bar{\Lambda}$  decayed at least 10 cm from the interaction point. Using somewhat wider cuts we then searched for a second  $\Lambda$  or  $\bar{\Lambda}$  in the same events. We obtained 10 events with both a  $\Lambda$  and a  $\bar{\Lambda}$  with an estimated background of  $1.6 \pm 0.5$  events and two events with two  $\Lambda$ 's with an estimated background of  $1.6 \pm 0.5$  events. After correcting for efficiency, acceptance and the unseen  $\Lambda(\bar{\Lambda})$  decay channels we obtained

$$\frac{\sigma(\Lambda\bar{\Lambda}+X)}{\sigma(\Lambda+X)+\sigma(\bar{\Lambda}+X)} = 0.22^{+0.13}_{-0.10}(\text{stat})^{+0.07}_{-0.05}(\text{syst})$$

where  $\sigma(\Lambda\bar{\Lambda}+X)$  is the inclusive cross section for producing a pair of baryons yielding  $\Lambda$  and  $\bar{\Lambda}$ , both lying in the momentum range 1–7 GeV/c, and  $\sigma(\Lambda+X)$ ,  $\sigma(\bar{\Lambda}+X)$  are the inclusive cross sections for producing baryons yielding  $\Lambda$  and  $\bar{\Lambda}$  respectively, the  $\Lambda$  or  $\bar{\Lambda}$  lying in the momentum range 1–7 GeV/c. Thus  $\sim 40\%$  of all baryons yielding  $\Lambda$  or  $\bar{\Lambda}$  in the momentum range 1–7 GeV/c have both strangeness and baryon number compensated by a baryon yielding a  $\bar{\Lambda}$  or  $\Lambda$  in that momentum range. The rapidity difference for the 10  $\Lambda\bar{\Lambda}$  pairs is shown in Fig. 11a. Of these 10 pairs, 1.6 are estimated to be background (i.e. containing two false or one false and one true  $\Lambda$  or  $\bar{\Lambda}$ ) and 1.3 are estimated to be true  $\Lambda\bar{\Lambda}$  pairs but coming from a false association of  $\Lambda$ ,  $\bar{\Lambda}$  from different baryon antibaryon pairs.

Using protons with  $p < 1.4$  GeV/c identified by time of flight we obtained 39 events with a  $\Lambda$  plus a  $\bar{p}$  (or  $\bar{\Lambda}+p$ ) and 17 events with a  $\Lambda$  plus a  $p$  (or  $\bar{\Lambda}+\bar{p}$ ). The rapidity difference for these pairs is shown in Fig. 11b. If we assume that the pairs with the same baryon number measure the uncorrelated background then the difference shown in Fig. 11c measures the rapidity difference when the baryon number of a  $\Lambda$  or  $\bar{\Lambda}$  is compensated by a  $\bar{p}$  or  $p$ .

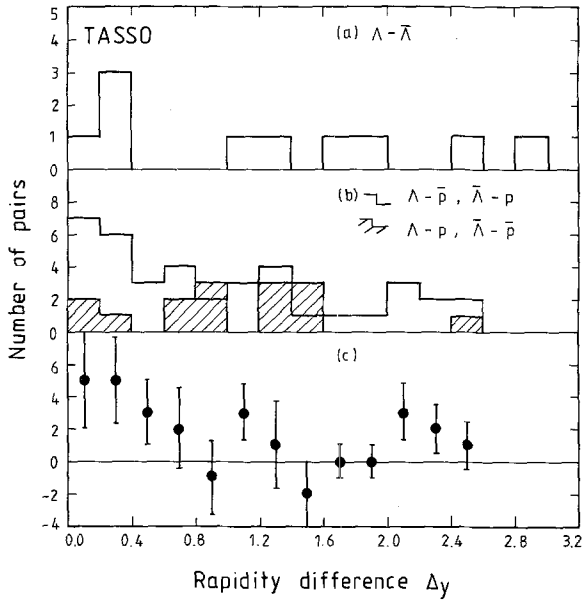


**Fig. 11.** **a** The rapidity difference between  $\Lambda$  and  $\bar{\Lambda}$  for events in which both are observed. **b** The rapidity difference between  $\Lambda$  and  $\bar{p}$  ( $\bar{\Lambda}$  and  $p$ ). The  $\Lambda p$  ( $\bar{\Lambda} \bar{p}$ ) rapidity difference is shown by the shaded plot. **c** The difference between the two histograms of **b**

## 8. Conclusions

We have measured differential and total cross sections for  $K^0$  and  $\Lambda$  production at  $W=14, 22$  and  $34$  GeV. The  $K^0$  data show some scale breaking. The total yield per event at the three  $W$  values was found to be  $1.15 \pm 0.10$ ,  $1.17 \pm 0.13$  and  $1.48 \pm 0.05$  for  $K^0$ 's and  $0.13 \pm 0.04$ ,  $0.22 \pm 0.05$  and  $0.31 \pm 0.03$  for  $\Lambda$ 's. Comparisons of the  $K^0$  and  $\Lambda$  data with results on  $\pi^\pm$ ,  $K^\pm$ ,  $p(\bar{p})$  and  $\Xi^-(\bar{\Xi}^-)$  production show a similar shape for the differential cross sections but a somewhat steeper increase in the total cross section with  $W$  for the higher mass particles. From the  $K^0$  data we obtain a value for the probability to produce strange quark-antiquark pairs relative to that to produce up or down quark-antiquark pairs during the fragmentation process of  $0.35 \pm 0.02 \pm 0.05$ . There is no evidence for  $\Lambda$  polarization in our data. We have measured  $p_T^2$  distributions with respect to the jet axis for both  $K^0$ 's and  $\Lambda$ 's and find that in the small  $p_T^2$  region both are well described by  $Ae^{(-p_T^2/2\sigma^2)}$  with  $\sigma=0.31 \pm 0.01$  GeV/c for  $K^0$ 's and  $\sigma$

$=0.38 \pm 0.04$  GeV/c for  $\Lambda$ 's. The comparable distribution for all charged particles shows a steeper rise at low  $p_T^2$  and does not follow this simple form. At large  $p_T^2$  there is a large tail in all three cases.

Apart from differences in rate, all the data are consistent with similar production mechanisms for strange and non-strange mesons and strange and non-strange baryons.

*Acknowledgements.* We thank the DESY directorate for their continuing support of the experiment and the PETRA machine group for their tremendous efforts. We thank the staff of the DESY Rechenzentrum, of the Rutherford Appleton Laboratory Computer Centre and of the HEP computers at Imperial College and Oxford Nuclear Physics Laboratory. Those of us from abroad wish to thank the DESY directorate for the hospitality extended to us while working at DESY.

## References

1. TASSO Collab. R. Brandelik et al.: Phys. Lett. **94B**, 91 (1980)
2. TASSO Collab. R. Brandelik et al.: Phys. Lett. **105B**, 75 (1981)
3. TASSO Collab. M. Althoff et al.: Z. Phys. C - Particles and Fields **17**, 5 (1983)
4. H. Aihara et al.: Phys. Rev. Lett. **52**, 577 (1984)
5. JADE Collab. W. Bartel et al.: Z. Phys. C - Particles and Fields **20**, 187 (1983)
6. PLUTO Collab. C. Berger et al.: Phys. Lett. **104B**, 79 (1981)
7. JADE Collab. W. Bartel et al.: Phys. Lett. **104B**, 325 (1981)
8. TASSO Collab. R. Brandelik et al.: Phys. Lett. **113B**, 499 (1982)
9. TASSO Collab. R. Brandelik et al.: Phys. Lett. **114B**, 65 (1982)
10. J.F. Patrick et al.: Phys. Rev. Lett. **49**, 1232 (1982)
11. TASSO Collab. M. Althoff et al.: Phys. Lett. **103B**, 340 (1983)
12. T. Sjöstrand: Comput. Phys. Commun. **27**, 243 (1982)
13. T. Sjöstrand: Comput. Phys. Commun. **28**, 229 (1983)
14. PLUTO Collab. J. Burmeister et al.: Phys. Lett. **67B**, 367 (1977)
15. V. Lüth et al.: Phys. Lett. **70B**, 120 (1977)
16. G.S. Abrams et al.: Phys. Rev. Lett. **44**, 10 (1980)
17. DASP Collab. R. Brandelik et al.: Nucl. Phys. **148B**, 189 (1979)
18. DASP Collab. R. Brandelik et al.: Phys. Lett. **76B**, 361 (1978)
19. A. Bartl, H. Fraas, W. Majerotto: Z. Phys. C - Particles and Fields **6**, 335 (1980)
20. J. Ranft, G. Ranft: Z. Phys. C - Particles and Fields **12**, 253 (1980)
21. S.L. Wu, G. Zobernig: Z. Phys. C - Particles and Fields **2**, 107 (1979)
22. M.S. Alam et al.: Phys. Rev. Lett. **53**, 24 (1984)